Taylor & Francis
Taylor & Francis Group

REPORT

ô OPEN ACCESS | Check for updates

Isolation of blood-brain barrier-crossing antibodies from a phage display library by competitive elution and their ability to penetrate the central nervous system

George Thom[a], Jon Hatcher[b], Arron Hearn[a], Judy Paterson[a], Natalia Rodrigo[a], Arthur Beljean[a], Ian Gurrell[b], and Carl Webster[a]

[a]Antibody Discovery and Protein Engineering, MedImmune, Cambridge, UK; [b]Neuroscience, IMED Biotech Unit, AstraZeneca, Cambridge, UK

ABSTRACT

The blood-brain barrier (BBB) is a formidable obstacle for delivery of biologic therapeutics to central nervous system (CNS) targets. Whilst the BBB prevents passage of the vast majority of molecules, it also selectively transports a wide variety of molecules required to maintain brain homeostasis. Receptor-mediated transcytosis is one example of a macromolecule transport system that is employed by cells of the BBB to supply essential proteins to the brain and which can be utilized to deliver biologic payloads, such as antibodies, across the BBB. In this study, we performed phage display selections on the mouse brain endothelial cell line, bEND.3, to enrich for antibody single-chain variable fragments (scFvs) that could compete for binding with a known BBB-crossing antibody fragment, FC5. A number of these scFvs were converted to IgGs and characterized for their ability to bind to mouse, rat and human brain endothelial cells, and subsequent ability to transport across the BBB. We demonstrated that these newly identified BBB-targeting IgGs had increased brain exposure when delivered peripherally in mice and were also able to transport a biologically active molecule, interleukin-1 receptor antagonist (IL-1RA), into the CNS. The antagonism of the interleukin-1 system within the CNS can result in the relief of neuropathic pain. We demonstrated that the BBB-targeting IgGs were able to elicit an analgesic response in a mouse model of nerve ligation-induced hypersensitivity when fused to IL-1RA.

Introduction

There has been substantial advancement of biologic-based therapeutics to 'block-buster' status over the last few decades, achieving profound clinical success for the treatment of inflammatory diseases and cancer.[1,2] However, the development of biologics as therapies for diseases involving the central nervous system (CNS) has proved much more challenging. This is in part due to poor brain penetration of large biologic molecules such as IgG. Around 0.1% of the injected dose of an IgG antibody reaches the brain following peripheral administration,[3] meaning that it is difficult to achieve sufficient concentration of antibody in the brain to elicit a therapeutic response. The development of CNS-penetrating delivery strategies to allow biologic targeting of central receptors at pharmacologically relevant levels is a key therapeutic goal for the biopharmaceutical industry in the treatment of many currently untreatable CNS conditions.

The blood-brain barrier (BBB) is the major impediment to the systemic treatment of CNS diseases because it functions as a physical, metabolic and immunological barrier protecting and regulating the homeostasis of the brain and preventing the free passage of molecules into the CNS.[4-6] However, in some areas of the brain, the BBB is less restrictive and allows the passage of hormones and nutrients from the blood to areas such as the hypothalamus, and the export of hormones to the pituitary.[7] Brain capillary

endothelial cells form the front line of the BBB and have specialized characteristics, such as tight junctions, which prevent paracellular transport of small and large (water soluble) compounds from the blood to the brain.[8-10] The capillary barrier features are maintained with the support of other cell types, such as astrocytes, perivascular neurons and pericytes.[11-13] This barrier allows the selective transport of essential molecules such as nutrients, signaling molecules and hormones, which is achieved via a series of specific transporters and receptors that regulate passage across brain capillary endothelial cells. Brain influx of nutrients and proteins such as iron,[14] insulin,[15] and leptin[16] occurs by a transcellular transport mechanism known as receptor-mediated transcytosis and is mediated by specific receptors.

The transporters and receptors involved in receptor-mediated transcytosis can be exploited for the transport of biologic drugs into the CNS by targeting them with antibodies and peptides that bind, undergo internalization, and can be transported across the cells of the barrier. This receptor-mediated transcytosis approach has become the principle means by which biologics are targeted to the CNS,[11,17] and a number of BBB-targeting technologies use receptor-mediated transcytosis to deliver payloads to the CNS through the targeting of transferrin receptor,[18-21] insulin receptor,[22] low-density lipoprotein receptor related protein-1[23] and CD98hca.[24]

FC5 is a camelid single domain antibody that is able to transcytose across the BBB[25, 26] and has been shown to deliver bioactive molecules to the CNS *in vivo*.[27,28] One of the advantages of FC5 is that it is species cross reactive and has demonstrated binding to rat, mouse and human brain endothelial cells.[25] Webster et al.[29] used a humanized version of FC5 (BBB-scFv or BBB-IgG) to demonstrate that FC5 could deliver an antibody antagonist of the metabotropic glutamate receptor-1 (mGluR1) across the BBB. After systemic administration, the BBB-mGluR1 bispecific antibody was detected in brain sections, internalized into brain vessels and bound to neuronal cells in the parenchyma. Furthermore, in a model of persistent inflammatory pain, peripherally administered BBB-mGluR1 bispecific antibody showed antagonism of mGluR1 centrally and elicited an analgesic response.[29] Whilst this antibody had the desired properties for BBB transport, it proved to be susceptible to proteolytic degradation, thus limiting its development for clinical use. We therefore sought to identify an antibody that binds to the same epitope, but that is derived from a fully human antibody library and has the requisite properties for clinical development.

We employed epitope competition selections on cells, where we isolated scFvs that showed competition for binding with BBB-IgG on brain capillary endothelial cells. Here, we have shown that those scFvs, once converted to IgG, possess the biophysical characteristics of a developable hIgG as well as the ability to cross the BBB and be readily detected in the central compartment. To confirm their utility for the delivery of biologic drugs, they were coupled to interleukin-1 receptor antagonist (IL-1RA), a potent antagonist of the IL-1 receptor signaling system, and tested in a model of neuropathic pain. Interleukin-1 (IL-1) is a pro-inflammatory cytokine involved in both normal homeostasis and in pathological conditions.[30] IL-1 expression is increased in conditions associated with pain and hyperalgesia.[31-33] Systemically applied IL-1 is a potent hyperalgesic,[34] and, when administered intrathecally, IL-1 drives allodynia and hyperalgesia.[35] However, there is a naturally occurring inhibitor of the pro-inflammatory effect of IL-1. IL-1RA that regulates and limits IL-1 signaling.[36] Blockade of IL-1 signaling with IL-1RA has been shown to provide analgesia in part due to a reduction in ectopic neuronal discharge[37] and can be used as a model molecule for determining the efficiency of transport across the BBB.[29] The IgGs evaluated in this study were able to elicit analgesia in the Seltzer model of neuropathic

pain when coupled to IL-1RA, confirming their ability to cross the BBB.

Results

Identification of FC5 mimetic IgGs

Phage display and in vitro binding of isolated scFvs/IgGs

Three naïve scFv phage libraries were utilized for cell selections on 10^7 bEND.3 cells with epitope competition using BBB-IgG.[29] After a preliminary round of enrichment of bEND.3 binding phage particles, two further rounds of competition selections were performed using 100 μM BBB-IgG to compete off any phage particles that displayed scFvs that bound to the same or over-lapping epitope as BBB-IgG.

BBB-IgG demonstrated concentration-dependent binding to bEND.3 cells as evaluated by FMAT and described in Webster et al.[26] In this study, the same FMAT assay was employed to perform single point screening of 8,000 scFv non-purified peri-plasmic-preparations isolated from the BBB-IgG competitive bEND.3 cell selections, using anti-HIS detection of the scFv c-terminal 6xHIS tag. scFvs that demonstrated positive binding to bEND.3 cells were taken forward for further profiling as purified scFv protein preparations (data not shown). A number of bEND.3-binding scFvs (numbered BBBtxxxx) were converted to human IgG1 format and subsequently demonstrated titratable binding to bEND.3 cells (Fig. 1A). These brain capillary endothelial cell binding IgGs also demonstrated species cross reactivity with titratable binding to primary rat brain capillary endothelial cells[38] (Fig. 1B) and a human brain capillary endothelial cell line (HCMEC/D3)[39] (Fig. 1C). An isotype control IgG, which binds to nitrophenol was employed in all three assays to demonstrate assay specificity for the binding of BBB-targeting IgGs.

Competition of BBBt scFvs with BBB-IgG

All scFvs that demonstrated titratable binding were assessed in a competition FMAT-based binding assay, whereby a constant concentration of scFv competed for binding to bEND.3 cells with increasing concentration of BBB-IgG. Where competition occurred, the fluorescent signal reduced as BBB-IgG concentration increased, and this was plotted as % maximal signal against BBB-IgG concentration (M) (Fig. 2). Eight scFv candidates demonstrated competitive binding with BBB-IgG, indicating
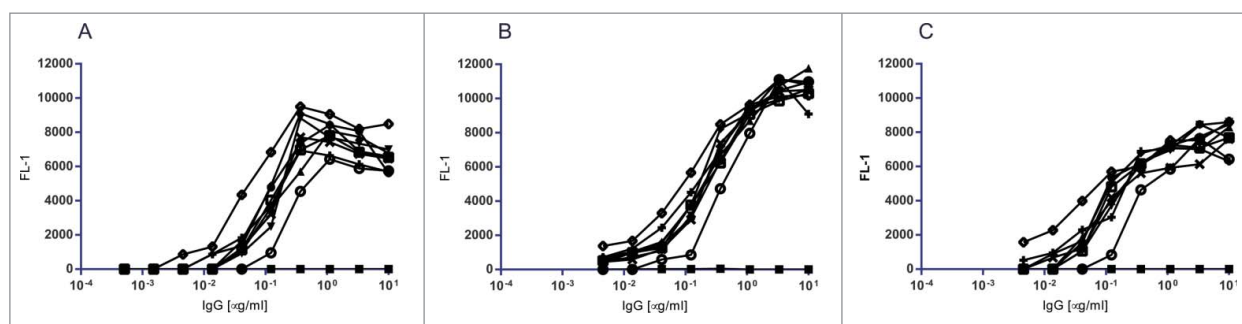

Figure 1. FMAT binding of BBB targeting hIgG1TM to brain capillary endothelial cells. FMAT binding assay to confirm the binding of BBB targeting hIgGs identified from epitope competition bEND.3 phage selections. FMAT assay binding curves of BBB hIgG1, BBB (○) and eight BBB targeting hIgGs, BBBt0626 (●), BBBt0632 (▼), BBBt0726 (▲), BBBt0654 (◆), BBBt0717 (◇), BBBt0727 (x), BBBt0732 (+), BBBt0754 (□) and isotype control hIgG1 (■). (A) BBB targeting hIgGs binding to mouse brain endothelial (bEND.3) cells (B) BBB targeting hIgGs binding to Rat Brain Capillary Endothelial Cells and (C) BBB targeting hIgGs binding to human D3 Brain Capillary Endothelial Cells.
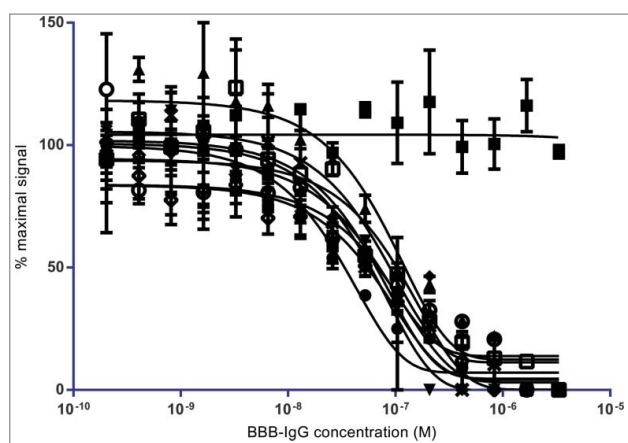
Figure 2. Competitive FMAT binding of lead BBB targeting scFvs to brain capillary endothelial cells: Competitive FMAT assay demonstrating the ability of isolated lead BBB targeting scFvs identified from FC5 epitope competition selections on bEND.3 cells to compete humanized FC5 BBB-hIgG binding. FC5 domain antibody, FC5 (○), BBBt0626 (●), BBBt0632 (▼), BBBt0726 (▲), BBBt0654 (♦), BBBt0717 (◊), BBBt0727 (x), BBBt0732 (+), and BBBt0754 (□) scFvs demonstrate reduced binding with increasing concentration of BBB-hIgG1. BBBt0734 (■) is shown as an example of a scFv for which binding is not affected by increasing concentration of BBB-hIgG1.

that they possessed a similar or overlapping epitope. However, there were several scFvs that, whilst able to specifically bind to bEND.3 cells, could not be competed off with excess BBB-IgG (Fig. 2).

Immunocytochemistry of BBBt-hIgG1s

The binding profile of the BBBt-hIgG1s was investigated by indirect immunocytochemistry on bEND.3 cells. Sub-confluent cultures of cells were fixed and permeabilized to mimic the conditions in which the antibodies were identified. BBB-hIgG1 demonstrated the strongest staining at the free edges of the bEND.3 cells and was also present in a punctate pattern throughout the cytoplasm (Fig. 3A). BBBt0626 and BBBt0632 exhibited a similar staining pattern, with BBBt0632 appearing to particularly pick out puncta surrounding the cell nuclei (Fig. 3B and C). The isotype control (NIP228) mAb did not show any specific staining in bEND.3 cells and gave a staining pattern identical to that obtained with the secondary detection antibody alone (Fig. 3E and E).

In vivo pharmacology pharmacokinetic properties of a BBB-targeting IgG

Peripheral PK

To confirm that the BBB-targeting IgGs isolated from bEND.3 cell competitive selections possessed improved brain exposure compared to control IgG, we conducted plasma pharmacokinetic (PK) and brain exposure studies in C57BL/6J mice. A 3-week *in vivo* plasma PK study was carried out in which mice were dosed with a single intravenous (i.v.) injection of one of three concentrations of BBBt0626 antibody (45, 4.5 or 0.45 mg/kg) followed by plasma sampling at regular intervals throughout the 3-week period. A control group received the same dosage of the control antibody (NIP228) of the same isotype as BBBt0626, but raised against an irrelevant antigen. Fig. 4A shows the mean plasma exposure profiles (μg/ml +/− standard error) of BBBt0626 BBB-targeting antibody and isotype control. There is little difference in the distribution (Vss) in plasma between BBBt0626 (0.07 +/− 0.02 L/Kg) and isotype control antibody (0.11 +/− 0.03 L/kg) or in plasma clearance of the two antibodies, with mean clearance values ranging between 6.4 (+/− 2.3) ml/day/kg for isotype control and 4.2 (+/− 0.5) ml/day/kg for BBBt0626, indicating that there is no significant antigen sink in the periphery for the BBB-targeting mAb in mouse.
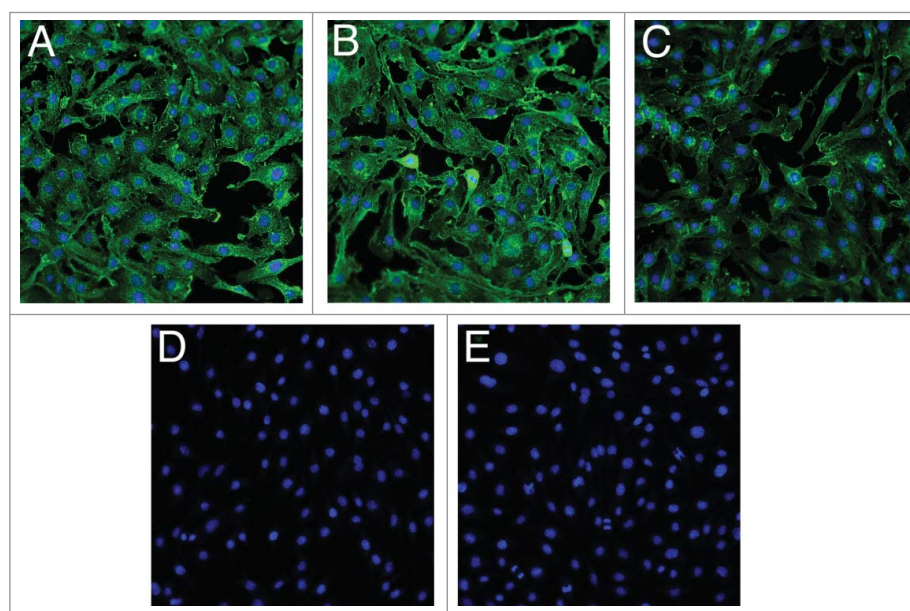
Figure 3. Indirect immunocytochemistry of lead BBB targeting hIgGs in bEND.3 cells. Images show fixed and permeabilized bEND.3 cells grown on collagen I-coated 96-well plates and stained with (A) BBB-IgG, (B) BBBt0626, (C) BBBt0632 and (D) Isotype control (NIP228). A secondary detection antibody alone control is shown in (E). Images are merged with Hoechst staining to show the position of the cell nuclei and are representative of 3 cultures, with four fields of view taken from each individual preparation of cells using the 20 × objective on an ImageXpress Micro XLS Wide Field High-Content Analysis System.

Figure 4. Pharmacokinetic determination of peripheral and brain drug levels following *i.v.* administration of isotype control and BBBt0626. C57BL/6 mice were injected via the tail ve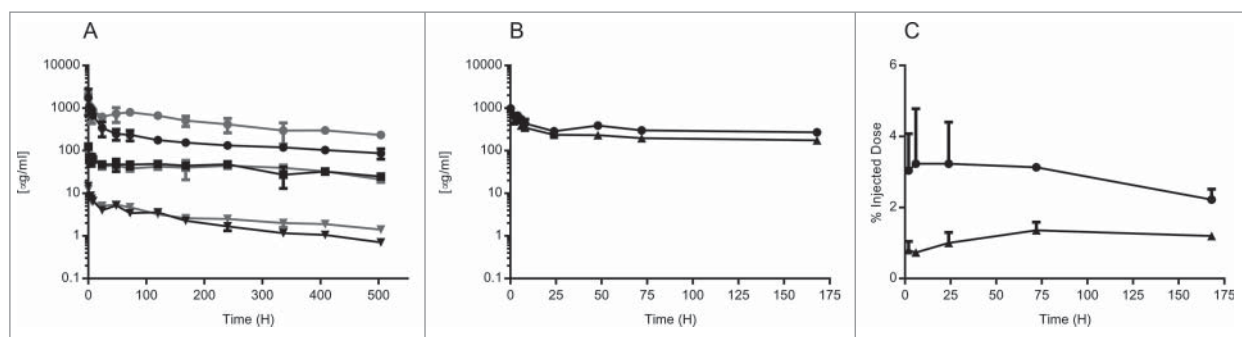in with BBB targeting hIgG1 antibody or isotype control antibody. Sampling was performed at regular intervals for either 1 or three weeks to determine plasma exposure for each antibody. (A) Comparison of 21 day plasma exposure (μg/ml) of isotype control (NIP228) at 0.45 mg/kg (▼) 4.5 mg/kg (■) and 45 mg/kg (●) or Bbbt0626 at 0.45 mg/kg (▼) 4.5 mg/kg (■) and 45 mg/kg (●). (B) Comparison of 7 day plasma exposure (μg/ml) of isotype control (▲) or Bbbt0626 (●) hIgG1TM. (C) Brain exposure of isotype control (▲) and BBBt0626 (●) as measured by % injected dose per g brain for 1 week.

Brain exposure

A brain exposure study was performed in which plasma- and capillary-depleted brain samples were taken from separate groups of mice at intervals throughout a 1-week period following a single i.v. dose of 30 mg/kg. The serial sampling procedure in this study resulted in composite profiles for plasma (Fig. 4B) and brain exposure (Fig. 4C). Each mouse provided two plasma sampling points, with the second sample being collected via cardiac puncture. After collection of the second sample, each animal remained under anesthesia, and phosphate-buffered saline (PBS) was infused via the heart's left ventricle. Mice were considered to be fully perfused after 10 ml PBS had been administered and the extremities (paws and ears) appeared white. Brains were carefully removed, scored and divided into two hemispheres. One hemisphere was flash frozen on dry-ice and the other was homogenized and processed to determine how much of the injected antibodies had reached the brain. Brain samples were taken at 2, 6, 24, 72 and 168 hours (hrs) post i.v. administration and processed to homogenate for analysis via MesoScale Discovery (MSD) assay. Cmax for both BBBt626 and the isotype control antibody in the plasma was observed at the earliest time point (2 hrs, Fig. 4B), whereas Cmax in the brain for BBBt0626 occurred at the 6 hr time point (Fig. 4C). BBBt0626 provided significantly higher brain exposure than isotype control, with between 2–3% injected dose observed throughout the 1-week period (Fig. 4C).

Analgesic effects of BBB-targeting-IL-1RA fusion molecules

In 1990, Seltzer et al described the development of a rodent neuropathic pain model, where there was an induced hypersensitivity phenotype in response to mechanical pressure at the ipsilateral paw. Webster et al.[40] further demonstrated that central delivery of interleukin-1 receptor antagonist (IL-1RA) could induce an analgesic response and reverse the hyperalgesia in this rodent neuropathic pain model.

Genetic fusions of either BBB-targeting or isotype control hIgG1TM with IL-1RA fused to the C-terminal end via a (Gly4Ser)3 flexible linker, were tested for their ability to induce analgesia in the neuropathic pain model following peripheral administration. All molecules were dosed at 40 mg/kg and operated (Op) animals undergoing partial nerve ligation were

compared to sham operated animals (Fig. 5). BBB-IL-1RA (Op+BBB) and BBBt0626-IL-1RA (Op+BBBt0626) both demonstrated partial but significant reversal of mechanical hyperalgesia at the 2-hr time-point, compared to control hIgG-IL-1RA (Op+control) or vehicle (Op+PBS) (Fig. 5). This was the first indication that these newly isolated BBB crossing antibody-IL-1RA genetic fusions were capable of transporting a therapeutic molecule from the periphery to the central compartment and eliciting an analgesic response in this pharmacodynamic model of hyperalgesia.

Subsequently, three BBB-targeting hIgGs (BBBt0626, BBBt0632 and BBBt0726) that had IL-1RA genetically fused to the C-terminus of the heavy chain were dosed at 100 mg/kg via sub cutaneous (*s.c.*) injection along with control groups containing vehicle or isotype control-IL-1RA fusion and monitored for 4 days post dose. Again, vehicle (Op+PBS) and isotype control-IL-1RA (Op+control) did not alter the level of mechanical hyperalgesia from pre-dose levels (Fig. 6A). However, all three BBBt antibody-fusions tested (BBBt0626, BBBt0632 and
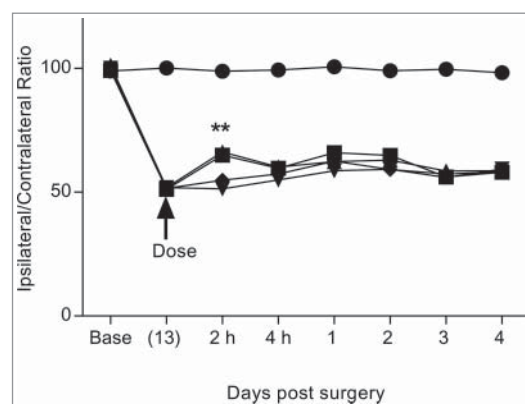
Figure 5. Comparison of *i.v.* dosed BBB targeting hIgG1TM-IL-1RA fusions in reversal of mechanical hyperalgesia in the Seltzer model of neuropathic pain. Compares the effect of *i.v.* dosed BBB-IgG and BBBt0626-IL-1RA fusion antibodies on reversal of PNL induced mechanical hyperalgesia by following the ratio of pressure applied to ipsilateral and contralateral hind paws. Sham + Control 40 mg/kg (●), Op + control 40 mg/kg (♦), Op + PBS 10 mg/kg (▼), Op + BBB 40 mg/kg (■) and Op + BBBt0626 40 mg/kg (▲). Sciatic nerve ligation surgery occurred at base (day 0) and IgG-IL-1RA fusion was administered 13 days post-surgery. Ipsilateral/contralateral ratio followed for a further 4 days. N = 10 per group. Data analyzed using 2-way ANOVA with time and treatment as dependent factors. Subsequent statistical significance obtained using Bonferroni's Post-Hoc test. **p < 0.01 to PNL/NIP-228/Kin control.

BBBt0726) produced statistically significant reversal of mechanical hyperalgesia from the first pain measurement point of 4 hrs through to the penultimate time-point at 2 days post dose (Fig. 6A). The magnitude of the response was very similar for all three BBBt-IL-1RA fusions tested. These results demonstrated that all three BBBt antibodies were able to transmigrate across the BBB and deliver their payload (IL-1RA) to the central compartment at a sufficient concentration to elicit an analgesic response. Furthermore, it was found that the analgesic response obtained with BBBt0626-IL-1RA was titratable and dependent on the amount that was peripherally administered (Fig. 6B). BBBt0626-IL-1RA (Op+BBBt0626) was dosed *i.v.* at 25, 50 and 100 mg/kg while the isotype control (Op+control), was dosed at the highest concentration (100 mg/kg). Vehicle and isotype control did not produce a reversal of mechanical hyperalgesia at any of the time points in this study. BBBt0626-IL-1RA, when dosed at 100 mg/kg, resulted in a statistically significant reversal of mechanical hyperalgesia from 2 hrs to 2 days post dose, but not at 4 days post dose. BBBt0626-IL-1RA when dosed at 50 mg/kg produced statistically significant analgesic effects at 2 hrs to 1 day post dose, and at 25 mg/kg

dosing resulted in a significant analgesic effect at 2–4 hrs post dose. These results demonstrated that higher peripheral dosing produced an increased and prolonged central analgesic response in this model of mechanical hyperalgesia.

Sustained analgesic effect with repeat dosing of BBBt0626 hIgG1TM-IL-1RA

Two experiments were performed to determine if multiple dosing of the BBBt0626-IL-1RA fusion could achieve a prolonged reversal of mechanical hyperalgesia. In the first multiple dose study, a second dose of 100 mg/kg was administered *s.c.* 24 hrs after the initial dose. This time point was chosen as the drug levels from the initial does were still high, and it avoided and excessive number of manipulations within the 24 hrs following dosing. The magnitude of the analgesic response following the second dose was increased to almost complete reversal of mechanical hyperalgesia (Fig. 6C). The length of the response extended to the end of the study, 4 days post second dose. In the second multiple dose study, the second dose of 100 mg/kg was administered 4 days after the initial dose when the analgesic response was starting to decline. Again, the magnitude of
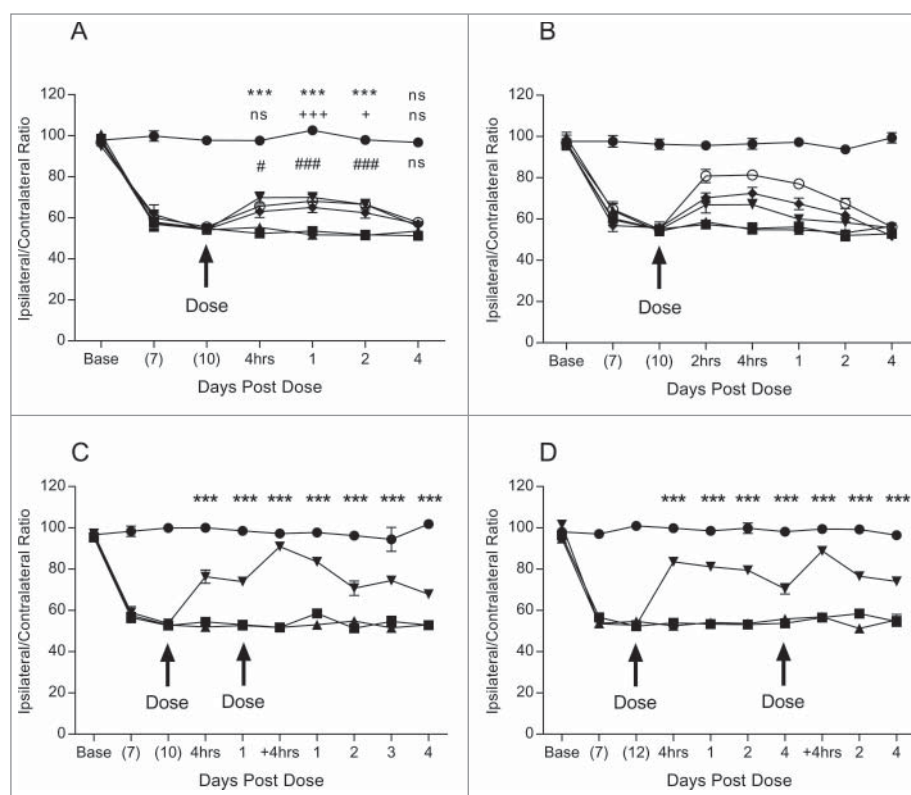

Figure 6. Pharmacodynamic analyses of lead BBB targeting hIgG1TM-IL-1RA fusions in Seltzer PNL model of mechanical hyperalgesia. Determination of the effect of *s.c.* dosed lead BBB-IL-1RA fusions (BBB-IL-1RA) on PNL induced mechanical hyperalgesia via measurement of the ratio of pressure applied to ipsilateral and contralateral hind paws. Sciatic nerve ligation surgery occurred at base (day 0) and BBB-IL-1RA administered 10 or 12 day post surgery. Ipsilateral/contralateral ratio was followed for a further 4 days. (A) Measurement of the analgesic effect of BBBt0626-IL-1RA 100 mg/kg (▼), BBBt0632-IL-1RA 100 mg/kg (♦) and BBBt0726-IL-1RA 100 mg/kg (○) compared to Op + isotype control-IL-1RA 100 mg/kg (▲) and Sham + PBS 10 ml/kg (●). N = 9–10 per group. Data analyzed using 2 way ANOVA with time and treatment as dependent factors. Subsequent statistical significance obtained using Tukey's Post Hoc test. *** $P<0.001$ Op + Control-IL-1RA vs Op + BBBt0626-IL-1RA; + $P<0.05$, +++ $P<0.001$ Op + Control-IL-1RA vs Op + BBBt0632-IL-1RA; # $P<0.05$, ### $P<0.001$ Op + Control-IL-1RA vs Op + BBBt0726-IL-1RA. (B) Analgesic effect of 100 (○), 50 (♦) and 25 mg/kg (▼) of BBBt0626-IL-1RA dosed *s.c.* compared to isotype control-IL-1RA at 100 mg/kg (▲) and Sham + PBS 10 ml/kg (●). N = 7–13 per group/time point. (C) Analgesic effect of a repeat dose of 100 mg/kg of BBBt0626-IL-1RA (▼) 24 h after initial dose when compared to isotype control-IL-1RA 100 mg/kg (▲), Op + PBS 10 ml/kg (■) and Sham + PBS 10 ml/kg (●). N = 8–10 per group. Data analyzed using 2-way ANOVA with time and treatment as dependent factors. Subsequent statistical significance obtained using Bonferroni's Post Hoc test. *** $P<0.001$ Op + Control-IL-1RA vs Op + BBBt0626-IL-1RA. (D) Analgesic effect of a repeat dose of 100 mg/kg of BBBt0626-IL-1RA (▼) 4 days after initial dose when compared to isotype control-IL-1RA 100 mg/kg (▲), Op + PBS 10 ml/kg (■) 10 and Sham + PBS 10 ml/kg (●). N = 9–10 per group. Data analyzed using 2-way ANOVA with time and treatment as dependent factors. Subsequent statistical significance obtained using Bonferroni's Post Hoc test. *** $P<0.001$ Op + Control-IL-1RA vs Op + BBBt0626-IL-1RA.

the analgesia provided almost complete reversal of the mechanical hyperalgesic response. The analgesic response continued for a further 4 days post second dose (Fig. 4D). These results tend to suggest that the IL-1RA analgesic response is not saturated after one *s.c.* dose of 100 mg/kg of BBBt-IL-1RA, which may be a feature of the PK of the molecule. More analysis would need to be performed to determine if this was the case.

Discussion

A number of studies have demonstrated that, by using receptor-mediated transcytosis, biologics can be transported across the BBB and reach the brain parenchyma. Recent studies[20, 21, 28, 29, 40] have exploited the receptor-mediated transcytosis pathways to cross the BBB and have demonstrated CNS delivery of large biologic entities, including antibodies that engage a CNS target, to potentially target currently intractable diseases of the CNS. However, in most cases the described antibodies do not bind the targeted receptor across multiple species, requiring different antibodies to be used for non-clinical and clinical studies.

FC5 is an exception to this trend, as it has been shown to cross the BBB *in vitro* and *in vivo* in several species.[25] A humanized FC5-derived IgG (BBB-hIgG1) that retained this species cross-reactivity was generated and demonstrated the ability to deliver an antibody antagonist of the metabotropic glutamate receptor-1 (BBB-mGluR1) to the central compartment.[29] Central mGluR1 target engagement after i.v. administration of BBB-mGluR1 was demonstrated by a dose-dependent inhibition of mGluR1-mediated thermal hyperalgesia in the Hargreaves pain model and by co-localization of the antibody with thalamic neurons involved with mGluR1-mediated pain processing. Ultimately, however, the BBB-hIgG1 antibody was deemed unsuitable for clinical studies because it lacked the developability properties necessary for a therapeutic molecule. However, its species cross-reactivity made it an attractive starting point for further antibody engineering.

In this study, we successfully isolated several human scFvs to the same or overlapping epitope as BBB-hIgG1 using competitive elution techniques on mouse brain endothelial cells. All of the subsequent BBBt antibodies tested showed binding to mouse, rat and human brain capillary endothelial cells. This species cross-reactivity and the possible flexibility of modularity (e.g., monovalent, bivalent, multivalent IgGs or scFvs) offered by the BBBt antibodies could more easily enable translational modelling and the subsequent development of BBB-permeable therapeutics for the treatment of CNS diseases.

Another advantage of the BBBt antibodies identified is their favorable plasma PK properties. A multi-dose level PK study in mice demonstrated that BBBt0626 had similar distribution and clearance phases to an isotype control antibody, indicating the lack of peripheral sink, which would lead to faster clearance. The importance of this feature is highlighted in previous studies using panels of anti-TfR antibodies with different receptor affinities. In two independent studies with different panels of anti-mouse TfR antibodies, the highest affinity antibody underwent much faster clearance than the lower affinity variants.[40, 41] In both studies, the higher affinity antibodies also showed the lowest levels of brain exposure. It is probable that

the higher affinity anti-TfR antibodies were undergoing rapid antigen-mediated clearance in the periphery, and were degraded in the lysosome together with the TfR in peripheral tissues expressing this receptor. At the BBB, high affinity binding to TfR could similarly result in degradation in the lysosome, which would negatively affect the level of antibody available for brain delivery. The PK profile observed for BBBt0626 suggests that there is limited antigen-mediated clearance of this antibody, which should ensure that the level of antigen available in the periphery is not a limiting factor in the uptake of antibody into the brain. However, the antigen for BBBt0626 has not yet been identified, therefore its levels in the periphery are not known. It is also not known if any shed forms of the antigen exist and whether or not they would influence the PK or brain distribution.

Demonstrating delivery of the BBBt molecules into the parenchyma of the brain is an important parameter because a centrally-acting therapeutic would have to reach this location to exert an effect, and there is evidence that some antibodies that target receptors on the surface of brain endothelial cells can become trapped on the cerebral vasculature, e.g., anti-TfR mAbs.[42] To this end, the brain samples used in our brain exposure assay were subjected to tissue homogenization and capillary depletion to remove any contaminating antibody trapped within the microvasculature. BBBt0626 was able to cross the BBB and accumulate in the brain more efficiently (∼3% injected dose per g tissue) than the same dose of isotype control mAb (NIP228) and for a prolonged period of time, with C_{max} occurring in the sample 6 hrs post dosing. These controlled data indicate transport of BBBt0626 into the brain parenchyma rather than it being sequestered on the microvessels of the brain.

To confirm central exposure of the BBBt antibodies, and to test whether they could deliver a therapeutic amount of active drug to the CNS following peripheral administration, fusions to IL-1RA were made. IL-1RA is a naturally occurring inhibitor that counteracts the pro-inflammatory effect of the cytokine IL-1.[36] IL-1 expression is increased in conditions associated with pain and hyperalgesia,[31-33] but blockade of IL-1 signaling with IL-1RA has been shown to result in analgesia, in part due to a reduction in ectopic neuronal discharge. It has previously been shown that, in a mouse model of neuropathic pain, symptoms can be relieved through central, but not peripheral blockade of IL-1R signaling.[37, 40] Using our BBBt-IL-1RA fusion molecules in this model of neuropathic pain, we demonstrated that our BBB-targeting mAbs, following peripheral administration (*i.v.* or *s.c.*), could deliver a pharmacologically active biologic payload (IL-1RA) to the CNS, resulting in an analgesic response by blockade of IL-1R signaling. The isotype control antibody IL-1RA fusion protein (NIP228-IL-1RA) did not induce analgesia in this model. The intensity and duration of analgesia was titratable in a dose-dependent manner. Furthermore, a second dose of the BBBt0626-IL-1RA fusion protein, either 1 or 4 days post initial dose resulted in more pronounced analgesia with prolonged duration suggesting that the transport pathway for BBBt0626 does not become saturated at these dose levels. In agreement with previous studies,[43,44] the data presented here suggest a role for central IL-1 in nociceptive signaling during chronic pain states. Greater IL-1RA penetration of

the CNS results in greater analgesia and prolonged exposure in the central compartment results in a longer duration of the analgesia induced by the IL-1RA fusion. The model has previously been used to demonstrate central delivery of IL-1RA using a reduced-affinity anti-TfR antibody[40] however this is the first demonstration of species cross-reactive, BBB-crossing, fully human antibodies that can deliver a pharmacologically active large biologic payload to the CNS and enhance its analgesic properties.

In both examples of IL-1RA delivery described here, the dose of the IgG-IL-1RA fusion required for an analgesic effect was large. There may be a number of reasons why this is the case. Whilst IL-1 has unequivocally been shown to be involved in the propagation of neuropathic pain, blockade of the IL-1 signaling pathway may not be the most efficacious method of reversing the pain phenotype. Additionally, the levels of BBBt0626 within the brain as measured by brain homogenization and ELISA represent an average of the level across the whole brain and may not reflect regional differences. Should the site of IL-1RA action be poorly served by this technology, reduced efficacy would result. Finally, we have not been able to determine whether the IgG-IL-1RA fusions remain intact, and loss of the IL-1RA portion of the molecule before it reached the site of action would reduce its effectiveness. Which one of these, or other factors, results in such a high dose being required is not clear, and further experimentation is needed before this approach becomes suitable for therapeutic use.

The importance of antibodies as a class of therapeutic drugs is now well established for cancer and inflammatory diseases,[1, 45] with Humira® (adalimumab) being the top-selling drug ($8.2 billion) in 2015. However, biologics such as antibodies or analgesic molecules do not cross the BBB in sufficient concentration to elicit an effect in CNS diseases and treatment of these conditions has remained elusive. Delivery of therapeutically relevant quantities, >0.1% injected dose across the BBB,[3] can only be achieved via the co-development of technologies that result in enhanced CNS penetration by the antibody, and in a format that will allow a subsequent increase in target engagement. Efficacy in the brain for biologics requires modification that would allow them to cross the BBB and subsequently to be released into brain parenchyma, providing access to their target cells at therapeutic levels, to elicit a disease-modifying pharmacological response. The engagement of their target at the BBB may result in modulation of the target through inhibition of ligand binding, or removal of the receptor due internalization and degradation. Caution is required in investigating new BBB transport pathways before the effect on the targeted receptor is known.

In conclusion, we demonstrated via *in vitro* cell binding data that we have identified a number of species cross-reactive BBB-targeting vectors (BBBts). We have shown, by plasma and brain pharmacokinetic analyses, that BBBt0626 is transported to the brain parenchyma and maintains good peripheral exposure. Also, we demonstrated that in a pharmacodynamic mouse model of neuropathic pain, a number of BBBt lead candidates were able to deliver therapeutic amounts of the analgesic protein IL-1RA to the CNS in a functionally active form where it was able to reverse mechanical hyperalgesia. These data indicate that BBBts have the potential as a delivery platform to transport therapeutic molecules to the CNS to treat a variety of CNS diseases and

conditions, enabling testing of the same molecule in rodent pre-clinical studies and clinical studies. However, further experimentation is required to demonstrate that these antibodies retain the same function in humans and non-human primates.

Materials and methods

Isolation of BBB-targeting scFvs by phage display and cell competitive selections

BBB-targeting scFvs were isolated from naïve libraries using modified phage display protocols.[46, 47] Briefly, 10^{12} purified phage particles for each library were incubated for one hr at room temperature with 10^7 prewashed and permeabilized (0.2% Triton in PBS for 15 minutes at room temperature) mouse brain endothelial (bEND.3) cells[48] in PBS pH 7.4 containing 3% skimmed milk powder. Following incubation, the cells were centrifuged at 1,000 x g in a benchtop centrifuge, the supernatant removed and cells re-suspended in PBS. This procedure was performed a further four times before phage particles were eluted from the cells with 0.1 M triethylamine (TEA). TEA ensured elution of internalized phage particles as well as those remaining on the surface of the cell. The eluted phage particles were allowed to infect mid-log phase growing *Escherichia coli* TG1 cells at 30°C and selection was applied by plating phage/*E. coli* suspension on 2TY agar with 100 μg/ml ampicillin and 2% glucose. Enriched phage particles from the first round of selection were amplified and prepared for the next round of selection on bEND.3 cells. During subsequent rounds of selection, 100 μM of BBB-IgG[29] was added to the cells instead of TEA and incubated for two hrs at room temperature. After incubation, phage particles present in the supernatant were recovered and allowed to infect mid-log *E. coli* TG1 cells. Two further rounds of competitive cell selections were performed before screening of individual scFvs from the selection outputs commenced. Crude bacterial periplasmic extracts (periprep) containing scFv antibodies from selection outputs were prepared in 50 mM 4-morpholinepropanesulfonic, 0.5 mM ethylenediaminetetraacetic acid (EDTA) and 500 mM sucrose pH 7.4 buffer according to a previously described method.[49]

Expression of scFv, IgG1 and IgG1-IL-1RA fusion molecules

ScFv expression and purification was performed as described by Dobson et al.[49] Briefly, *E. coli* TG1 cells containing plasmids expressing the scFv of interest were cultured in 2TY media at 37°C, expression was induced with 1 mM isopropyl β-D-1-thiogalactoside, and scFv proteins were isolated from the periplasm by osmotic shock using 50 mM Tris-HCl, 0.5 mM EDTA, 500 mM sucrose (TES) pH 7.4 buffer. If required, scFvs were further purified by nickel affinity chromatography.

The scFvs were converted to human IgG1 molecules essentially as described by Persic et al.[50] with the Fc domain containing the mutations S239D/A330L/I332E to eliminate effector function (IgG1 TM;)[51] IgG molecules were expressed in Chinese hamster ovary cells in serum-free media as previously described.[52] Cultures were maintained in a humidified incubator at 37°C, 5% CO_2 for 14 days after which the medium was harvested. Antibodies were purified from cell culture media using protein A affinity chromatography followed by size-

exclusion chromatography. The concentration of IgG was determined spectrophotometrically using an extinction coefficient based on the amino acid sequence of the IgG.[53]

Plasmids encoding IL-1RA fused to the C-terminus of the IgG1 TM heavy chain via a $(G_4S)_3$ linker were assembled by polymerase chain reaction (PCR) amplification of the IL-1RA gene from cDNA obtained from Source Bioscience (Nottingham, UK) and subsequent PCR amplification with oligos that overlapped the IL-1RA gene and the IgG1 TM CH3 domain and incorporated the linker. Expression and purification of IgG1 TM-IL-1RA fusions was performed as described above.

Cell binding assays

Fluorescence microvolume assay technology (FMAT)

Cell binding was assessed by the method of Miraglia et al.[54] using Fluorescence Microvolume Assay Technology (FMAT). bEND.3 cells were obtained from the European Collection of Authenticated Cultures (ECACC) and were maintained in Dulbecco's Modified Eagle Medium supplemented with 10% fetal bovine serum. Cells were used between passages 4 and 20.

Periprep extract or Nickel-purified scFvs from *E. coli* were transferred into assay plates (Costar #3655) containing 10 μl (1:1000 dilution of a 1 mg/ml stock solution) mouse anti-HIS MAb (Advanced Targeting Systems #AB-213) and 10 μl (1:500 dilution of 2 mg/ml stock) goat anti-mouse AF647 MAb (Invitrogen) in FMAT buffer (Dulbecco's PBS, 0.1% bovine serum albumin (BSA; Sigma #A9576) and 0.01% sodium azide, pH7.4). bEND.3 cells[48] resuspended in FMAT buffer were added to plates and incubated for 2–5 hrs at room temperature. Plates were read on the Applied Biosystems Cellular Detection System 8200 and data analyzed using the Velocity algorithm with appropriate gating. ScFvs demonstrating similar binding characteristics to FC5/BBB were identified for further analysis. Second line FMAT binding assays were also employed to determine species cross reactivity of any scFvs identified in the bEND.3 FMAT binding assay, whereby binding to primary rat brain capillary endothelial cells[38] and a human brain capillary endothelial cell line (HCMEC/D3)[39] were assessed.

hIgG1TM or hIgG1TM-IL-1RA cell binding was assessed as above with the following change: Detection of hIgG1 TM proteins was with 10 μl Alexa Fluor 647-labelled goat anti-human IgG (H+L) (ThermoFisher Scientific #A-21445) diluted to 1.5 μg/ml in FMAT buffer.

Competition FMAT assay

Competition FMAT assays were carried out as above for the cell binding assays but with the addition of a 1 in 2 dilution series of BBB-IgG (commencing at 3.33 μM). Each well contained 10 μl scFv of interest (40 μg/ml), 10 μl mouse anti-HIS MAb (1 μg/ml), 10 μl Alexa Fluor 647-labelled goat anti-mouse (4 μg/ml), 10 μl BBB-IgG and 10 μl bEND.3 cells (4.0 $\times$ 10^5 cells/ml). Competition was indicated by a reduction in Alexa Fluor 647 signal. ScFvs that competed with BBB-IgG binding on bEND.3 cells were selected for subsequent analysis.

Immunocytochemistry

bEND.3 cells were seeded into collagen 1-coated 96-well μClear plates (Greiner Bio-One) and cultured overnight at 37°C, 5% CO_2. Cells were fixed with 3.7% formaldehyde for 20 minutes at room temperature followed by permeabilization with 0.2% Triton X-100 in PBS for five minutes. After rinsing once in PBS, cells were blocked in 3% BSA in PBS overnight. All primary antibodies were diluted to working concentration in 1% BSA in PBS. Cells were incubated with primary antibody for one hr at room temperature, followed by three 5 minute washes in PBS. Alexa Fluor 488 Goat anti-human pAb – F(ab')2 polyclonal Fc-specific (ThermoFisher Scientific #H10120) was used as the secondary detection antibody and diluted 1:2000 in 1% BSA/PBS. Cells were incubated with secondary antibody for one hr at room temperature followed by three 5 minute washes in PBS. Cells were counter-stained with Hoechst 33342 trihydrochloride, trihydrate (ThermoFisher Scientific), diluted to 1 μg/mL in 1% BSA/PBS, for one minute and rinsed a further three times in PBS. Samples were imaged using an ImageXpress Micro XLS Wide Field High-Content Analysis System (Molecular Devices).

Partial nerve ligation

Partial nerve ligation studies were performed as described in Webster et al.[40] Briefly, all studies were performed using adult female C57Bl/6J mice weighing 18–22 g (Charles River, UK). All procedures were performed in accordance with the Animals (Scientific Procedures) Act 1986 and were approved by a local ethics committee. All mice underwent insertion of transponders under anesthesia (3% isoflurane in oxygen) for identification purposes at least five days before the start of each study. Mechanical hyperalgesia was determined using an analgysemeter.[43] An increasing force was applied to the dorsal surface of each hind paw in turn until a withdrawal response was observed. The application of force was halted at this point and the weight in grams recorded. Data was expressed as withdrawal threshold in grams for ipsilateral and contralateral paws. Following the establishment of baseline readings, mice were divided into 2 groups with approximately equal ipsilateral/contralateral ratios and subsequently either underwent surgery to partially ligate the sciatic nerve or served as sham operated controls based on the previously described method of Seltzer et al. Mice were anesthetized with isoflurane and approximately 1 cm of the left sciatic nerve exposed by blunt dissection through an incision at the level of the mid-thigh. A suture (9/0 Virgin Silk: Ethicon) was passed through the dorsal third of the nerve and tied tightly. The incision was closed using Vetbond and the mice were allowed to recover for at least seven days prior to commencement of testing. Sham-operated mice underwent the same protocol but, following exposure of the nerve, the mice were glued and allowed to recover. Mice were tested for baseline responses on day 7 and day 10 post surgery. Operated mice showing ipsilateral/contralateral ratios of greater than 80% were classed as non-responders and were removed from the study. The remaining mice were then randomly allocated into treatment groups of 8–10 mice per group with approximately equal ipsilateral/contralateral ratios, following which mice were treated with the compound under test. Sham-operated animals received PBS vehicle (10 ml/kg). To investigate the effects of the BBB fusions, animals received PBS vehicle (10 ml/kg bodyweight *s.c.* or *i.v.*), isotype control

antibody IL-1RA fusion or the relevant BBBt antibody-IL-1RA fusion protein (25 to 100 mg/kg *s.c.* or *i.v.*). Sham-operated mice received PBS vehicle (10 ml/kg bodyweight s.c. or i.v.). Mice were re-tested for changes in mechanical hyperalgesia 2 hrs or 4 hrs post dose as previously described. Mice were also re-tested at 1, 2, 3 and 4 days post dose.

Data analysis

Statistical analysis was performed in GraphPad Prism. Only animals that completed the study were included in the analysis. Results were analyzed using 2-way ANOVA. Subsequent statistical significance obtained using Bonferroni's Post hoc test.

Peripheral kinetics and brain exposure

All studies to measure antibody exposure in the periphery and brain were performed at Quotient Biosciences (Newmarket, UK). Male C57B/6 mice, age 10–12 weeks, were intravenously injected with BBBt0626 or control IgG at 45, 30, 4.5 and 0.45 mg/kg. I.v. doses were administered into a tail vein at a constant dose volume of 10 ml/kg. Antibodies were supplied in D-PBS (Sigma). Following dosing, two blood plasma samples were collected into individual Li-Heparin containers from each of between four and six animals per time point per dose group. The first sample from each animal was collected from the lateral tail vein (*ca* 200 μl) into a Li-Hep microvette (BD Diagnostic Systems), while the second sample (*ca* 600 μl) was collected by cardiac puncture under isoflurane anesthesia into a Li-hep microtainer (BD Diagnostic Systems). Following collection, blood samples were allowed to clot for 30 minutes and centrifuged at 10,000 x g for 2 minutes at 4°C and the resultant plasma drawn off. Plasma samples were flash frozen on dry ice for subsequent analysis. After final blood collection, the mice were perfused with D-PBS at a rate of 2 ml/min for 10 minutes until the extremities appeared white. Brains were excised and one hemisphere was snap frozen in liquid nitrogen, and the other immediately processed.

The brain hemisphere was homogenized in five volumes of ice-cold PBS containing 0.5% Tween 20 and Complete® protease inhibitor cocktail tablets (Roche Diagnostics). Homogenization was performed in a 10 ml Potter-Elvehjem mortar type glass homogenizer with PTFE pestle, using 2 × 10 clockwise strokes with 5 second rest time. Homogenates were transferred to LoBind tubes (Eppendorf) and rotated at 4°C for one hr before centrifuging in a chilled bench-top centrifuge at 13,000 x g for 20 minutes. The capillary-depleted supernatant was isolated for brain antibody measurement.

Measurement of antibody concentrations in mouse brain and plasma

Antibody concentrations in mouse plasma and brain samples were measured via MSD assay platform. The MSD employs a plate-based sandwich immunoassay format where anti-human IgG capture antibody binds calibrator or samples, and a specific anti-human IgG detection antibody labelled with SULFO-TAG emits light upon electrochemical stimulation. Levels of BBB-targeting and control antibody in plasma and brain samples were quantified by reference to standard curves generated using calibrator samples with a four-parameter nonlinear regression model.

Abbreviations

BBB	Blood-Brain Barrier
CNS	Central Nervous System
EDTA	Ethylenediaminetetraacetic acid
FMAT	Fluorescent Microvolume Assay Technology
HCMEC/D3	Human Cerebral Microvascular Endothelial Cells- D3
IgG	Immunoglobulin G
IL-1	Interleukin 1
IL-1RA	Interleukin 1 Receptor Antagonist
i.v.	Intravenous
mAb	Monoclonal Antibody
mGluR1	Metabotropic Glutamate Receptor-1
MSD	MesoScale Discovery
Op	Operated
PBS	Phosphate-Buffered Saline
PCR	Polymerase Chain Reaction
PK	Pharmacokinetic
s.c.	Subcutaneous
ScFv	Single-Chain Fragment variable
TEA	Triethylamine
TfR	Transferrin Receptor
2TY	2xTryptone Yeast Extract

References

1. Beck A, Wurch T, Bailly C, Corvaia N. Strategies and challenges for the next generation of therapeutic antibodies. Nat Rev Immunol. 2010;10:345–52. doi:10.1038/nri2747.
2. Ayyar BV, Arora S, O'Kennedy R. Coming-of-Age of Antibodies in Cancer Therapeutics. Trends Pharmacol Sci. 2016;37:1009–28. doi:10.1016/j.tips.2016.09.005.
3. Boado RJ, Zhou QH, Lu JZ, Hui EK, Pardridge WM. Pharmacokinetics and brain uptake of a genetically engineered bifunctional fusion

antibody targeting the mouse transferrin receptor. Mol Pharm. 2010;7:237–44. doi:10.1021/mp900235k.

4. Gaillard PJ, de Boer AB, Breimer DD. Pharmacological investigations on lipopolysaccharide-induced permeability changes in the blood-brain barrier in vitro. Microvasc Res. 2003;65:24–31. doi:10.1016/S0026-2862(02)00009-2.

5. Abbott NJ, Patabendige AA, Dolman DE, Yusof SR, Begley DJ. Structure and function of the blood-brain barrier. Neurobiol Dis. 2010;37:13–25. doi:10.1016/j.nbd.2009.07.030.

6. Abbott NJ, Friedman A. Overview and introduction: the blood-brain barrier in health and disease. Epilepsia. 2012;53(Suppl 6):1–6. doi:10.1111/j.1528-1167.2012.03696.x.

7. Haddad-Tovolli R, Dragano NRV, Ramalho AFS, Velloso LA. Development and Function of the Blood-Brain Barrier in the Context of Metabolic Control. Front Neurosci. 2017;11:224. doi:10.3389/fnins.2017.00224.

8. Brightman MW, Reese TS. Junctions between intimately apposed cell membranes in the vertebrate brain. J Cell Biol. 1969;40:648–77. doi:10.1083/jcb.40.3.648.

9. Reese TS, Karnovsky MJ. Fine structural localization of a blood-brain barrier to exogenous peroxidase. J Cell Biol. 1967;34:207–17. doi:10.1083/jcb.34.1.207.

10. Bauer H, Traweger A. Tight Junctions of the Blood-Brain Barrier – A Molecular Gatekeeper. CNS Neurol Disord Drug Targets. 2016;15:1016–29. doi:10.2174/1871527315666160915142244.

11. Pardridge WM. Drug and gene delivery to the brain: the vascular route. Neuron. 2002;36:555–8. doi:10.1016/S0896-6273(02)01054-1.

12. Abbott NJ, Ronnback L, Hansson E. Astrocyte-endothelial interactions at the blood-brain barrier. Nat Rev Neurosci. 2006;7:41–53. doi:10.1038/nrn1824.

13. Zlokovic BV. The blood-brain barrier in health and chronic neurodegenerative disorders. Neuron. 2008;57:178–201. doi:10.1016/j.neuron.2008.01.003.

14. Jefferies WA, Brandon MR, Hunt SV, Williams AF, Gatter KC, Mason DY. Transferrin receptor on endothelium of brain capillaries. Nature. 1984;312:162–3. doi:10.1038/312162a0.

15. Duffy KR, Pardridge WM. Blood-brain barrier transcytosis of insulin in developing rabbits. Brain Res. 1987;420:32–8. doi:10.1016/0006-8993(87)90236-8.

16. Golden PL, Maccagnan TJ, Pardridge WM. Human blood-brain barrier leptin receptor. Binding and endocytosis in isolated human brain microvessels. J Clin Invest. 1997;99:14–8. doi:10.1172/JCI119125.

17. Lajoie JM, Shusta EV. Targeting receptor-mediated transport for delivery of biologics across the blood-brain barrier. Annu Rev Pharmacol Toxicol. 2015;55:613–31. doi:10.1146/annurev-pharmtox-010814-124852.

18. Lee HJ, Engelhardt B, Lesley J, Bickel U, Pardridge WM. Targeting rat anti-mouse transferrin receptor monoclonal antibodies through blood-brain barrier in mouse. J Pharmacol Exp Ther. 2000;292:1048–52.

19. Zhang Y, Pardridge WM. Blood-brain barrier targeting of BDNF improves motor function in rats with middle cerebral artery occlusion. Brain Res. 2006;1111:227–9. doi:10.1016/j.brainres.2006.07.005.

20. Yu YJ, Zhang Y, Kenrick M, Hoyte K, Luk W, Lu Y, Atwal J, Elliott JM, Prabhu S, Watts RJ, et al. Boosting brain uptake of a therapeutic antibody by reducing its affinity for a transcytosis target. Sci Transl Med. 2011;3:84ra44. doi:10.1126/scitranslmed.3002230.

21. Niewoehner J, Bohrmann B, Collin L, Urich E, Sade H, Maier P, Rueger P, Stracke JO, Lau W, Tissot AC, et al. Increased brain penetration and potency of a therapeutic antibody using a monovalent molecular shuttle. Neuron. 2014;81:49–60. doi:10.1016/j.neuron.2013.10.061.

22. Boado RJ, Zhang Y, Zhang Y, Pardridge WM. Humanization of anti-human insulin receptor antibody for drug targeting across the human blood-brain barrier. Biotechnol Bioeng. 2007;96:381–91. doi:10.1002/bit.21120.

23. Demeule M, Currie JC, Bertrand Y, Ché C, Nguyen T, Régina A, Gabathuler R, Castaigne JP, Béliveau R. Involvement of the low-density lipoprotein receptor-related protein in the transcytosis of the

brain delivery vector angiopep-2. J Neurochem. 2008;106:1534–44. doi:10.1111/j.1471-4159.2008.05492.x.

24. Zuchero YJ, Chen X, Bien-Ly N, Bumbaca D4 Tong RK, Gao X, Zhang S, Hoyte K, Luk W, Huntley MA, et al. Discovery of Novel Blood-Brain Barrier Targets to Enhance Brain Uptake of Therapeutic Antibodies. Neuron. 2016;89:70–82. doi:10.1016/j.neuron.2015.11.024.

25. Muruganandam A, Tanha J, Narang S, Stanimirovic D. Selection of phage-displayed llama single-domain antibodies that transmigrate across human blood-brain barrier endothelium. FASEB J. 2002;16:240–2.

26. Abulrob A, Sprong H, Van Bergen en Henegouwen P, Stanimirovic D. The blood-brain barrier transmigrating single domain antibody: mechanisms of transport and antigenic epitopes in human brain endothelial cells. J Neurochem. 2005;95:1201–14. doi:10.1111/j.1471-4159.2005.03463.x.

27. Haqqani AS, Caram-Salas N, Ding W, Brunette E, Delaney CE, Baumann E, Boileau E, Stanimirovic D. Multiplexed evaluation of serum and CSF pharmacokinetics of brain-targeting single-domain antibodies using a NanoLC-SRM-ILIS method. Mol Pharm. 2013;10:1542–56. doi:10.1021/mp3004995.

28. Farrington GK, Caram-Salas N, Haqqani AS, Brunette E, Eldredge J, Pepinsky B, Antognetti G, Baumann E, Ding W, Garber E, et al. A novel platform for engineering blood-brain barrier-crossing bispecific biologics. FASEB J. 2014;28:4764–78. doi:10.1096/fj.14-253369.

29. Webster CI, Caram-Salas N, Haqqani AS, Thom G, Brown L, Rennie K, Yogi A, Costain W, Brunette E, Stanimirovic DB. Brain penetration, target engagement, and disposition of the blood-brain barrier-crossing bispecific antibody antagonist of metabotropic glutamate receptor type 1. FASEB J. 2016;30:1927–40. doi:10.1096/fj.201500078.

30. Dinarello CA. Biologic basis for interleukin-1 in disease. Blood. 1996;87:2095–147.

31. Alexander GM, van Rijn MA, van Hilten JJ, Perreault MJ, Schwartzman RJ. Changes in cerebrospinal fluid levels of pro-inflammatory cytokines in CRPS. Pain. 2005;116:213–9. doi:10.1016/j.pain.2005.04.013.

32. Apkarian AV, Lavarello S, Randolf A, Berra HH, Chialvo DR, Besedovsky HO, del Rey A. Expression of IL-1beta in supraspinal brain regions in rats with neuropathic pain. Neurosci Lett. 2006;407:176–81. doi:10.1016/j.neulet.2006.08.034.

33. del Rey A, Apkarian AV, Martina M, Besedovsky HO. Chronic neuropathic pain-like behavior and brain-borne IL-1beta. Ann N Y Acad Sci. 2012;1262:101–7. doi:10.1111/j.1749-6632.2012.06621.x.

34. Ferreira SH, Lorenzetti BB, Bristow AF, Poole S. Interleukin-1 beta as a potent hyperalgesic agent antagonized by a tripeptide analogue. Nature. 1988;334:698–700. doi:10.1038/334698a0.

35. Reeve AJ, Patel S, Fox A, Walker K, Urban L. Intrathecally administered endotoxin or cytokines produce allodynia, hyperalgesia and changes in spinal cord neuronal responses to nociceptive stimuli in the rat. Eur J Pain. 2000;4:247–57. doi:10.1053/eujp.2000.0177.

36. Carter DB, Deibel MR Jr, Dunn CJ, Tomich CS, Laborde AL, Slightom JL, Berger AE, Bienkowski MJ, Sun FF, McEwan RN, et al. Purification, cloning, expression and biological characterization of an interleukin-1 receptor antagonist protein. Nature. 1990;344:633–8. doi:10.1038/344633a0.

37. Gabay E, Wolf G, Shavit Y, Yirmiya R, Tal M. Chronic blockade of interleukin-1 (IL-1) prevents and attenuates neuropathic pain behavior and spontaneous ectopic neuronal activity following nerve injury. Eur J Pain. 2011;15:242–8. doi:10.1016/j.ejpain.2010.07.012.

38. Watson PM, Paterson JC, Thom G, Ginman U, Lundquist S, Webster CI. Modelling the endothelial blood-CNS barriers: a method for the production of robust in vitro models of the rat blood-brain barrier and blood-spinal cord barrier. BMC Neurosci. 2013;14:59. doi:10.1186/1471-2202-14-59.

39. Weksler BB, Subileau EA, Perriere N, Charneau P, Holloway K, Leveque M, Tricoire-Leignel H, Nicotra A, Bourdoulous S, Turowski P, et al. Blood-brain barrier-specific properties of a human adult brain endothelial cell line. FASEB J. 2005;19:1872–4.

40. Webster CI, Hatcher J, Burrell M, Thom G, Thornton P, Gurrell I, Chessell I. Enhanced delivery of IL-1 receptor antagonist to the central nervous system as a novel anti-transferrin receptor-IL-1RA fusion

reverses neuropathic mechanical hypersensitivity. Pain. 2017; 158:660–8. doi:10.1097/j.pain.0000000000000810.

41. Couch JA, Yu YJ, Zhang Y, Tarrant JM, Fuji RN, Meilandt WJ, Solanoy H, Tong RK, Hoyte K, Luk W, et al. Addressing safety liabilities of TfR bispecific antibodies that cross the blood-brain barrier. Sci Transl Med. 2013;5:183ra157, 181–112. doi:10.1126/scitranslmed.3005338.

42. Paris-Robidas S, Emond V, Tremblay C, Soulet D, Calon F. In vivo labeling of brain capillary endothelial cells after intravenous injection of monoclonal antibodies targeting the transferrin receptor. Mol Pharmacol. 2011;80:32–39. doi:10.1124/mol.111.071027.

43. Fiorentino PM, Tallents RH, Miller JN, Brouxhon SM, O'Banion MK, Puzas JE, Kyrkanides S. Spinal interleukin-1beta in a mouse model of arthritis and joint pain. Arthritis Rheum. 2008;58:3100–09. doi:10.1002/art.23866.

44. Zhang RX, Li A, Liu B, Wang L, Ren K, Zhang H, Berman BM, Lao L. IL-1ra alleviates inflammatory hyperalgesia through preventing phosphorylation of NMDA receptor NR-1 subunit in rats. Pain. 2008;135:232–9. doi:10.1016/j.pain.2007.05.023.

45. Wang S, Jia M. Antibody Therapies in Cancer. Adv Exp Med Biol. 2016;909:1–67. doi:10.1007/978-94-017-7555-7_1.

46. Vaughan TJ, Williams AJ, Pritchard K, Osbourn JK, Pope AR, Earnshaw JC, McCafferty J, Hodits RA, Wilton J, Johnson KS. Human antibodies with sub-nanomolar affinities isolated from a large non-immunized phage display library. Nat Biotechnol. 1996;14:309–14. doi:10.1038/nbt0396-309.

47. Lloyd C, Lowe D, Edwards B, Welsh F, Dilks T, Hardman C, Vaughan T. Modelling the human immune response: performance of a 1011 human antibody repertoire against a broad panel of therapeutically relevant antigens. Protein Eng Des Sel. 2009;22:159–68. doi:10.1093/protein/gzn058.

48. Montesano R, Pepper MS, Mohle-Steinlein U, Risau W, Wagner EF, Orci L. Increased proteolytic activity is responsible for the aberrant morphogenetic behavior of endothelial cells expressing the middle T oncogene. Cell. 1990;62:435–45. doi:10.1016/0092-8674(90)90009-4.

49. Dobson CL, Main S, Newton P, Chodorge M, Cadwallader K, Humphreys R, Albert V, Vaughan TJ, Minter RR, Edwards BM. Human monomeric antibody fragments to TRAIL-R1 and TRAIL-R2 that display potent in vitro agonism. mAbs. 2009;1:552–62. doi:10.4161/mabs.1.6.10057.

50. Persic L, Roberts A, Wilton J, Cattaneo A, Bradbury A, Hoogenboom HR. An integrated vector system for the eukaryotic expression of antibodies or their fragments after selection from phage display libraries. Gene. 1997;187:9–18. doi:10.1016/S0378-1119(96)00628-2.

51. Oganesyan V, Gao C, Shirinian L, Wu H, Dall'Acqua WF. Structural characterization of a human Fc fragment engineered for lack of effector functions. Acta Crystallogr D Biol Crystallogr. 2008;64:700–04. doi:10.1107/S0907444908007877.

52. Daramola O, Stevenson J, Dean G, Hatton D, Pettman G, Holmes W, Field R. A high-yielding CHO transient system: coexpression of genes encoding EBNA-1 and GS enhances transient protein expression. Biotechnol Prog. 2014;30:132–41. doi:10.1002/btpr.1809.

53. Pace CN, Vajdos F, Fee L, Grimsley G, Gray T. How to measure and predict the molar absorption coefficient of a protein. Protein Sci. 1995;4:2411–23. doi:10.1002/pro.5560041120.

54. Miraglia S, Swartzman EE, Mellentin-Michelotti J, Evangelista L, Smith C, Gunawan II, Lohman K, Goldberg EM, Manian B, Yuan PM. Homogeneous Cell- and Bead-Based Assays for High Throughput Screening Using Fluorometric Microvolume Assay Technology. J Biomol Screen. 1999;4:193–204. doi:10.1177/108705719900400407.